

## Ratiometric Fluorescent Sensor Proteins with Subnanomolar Affinity for Zn(II) Based on Copper Chaperone Domains

Elisabeth M. W. M. van Dongen,<sup>†</sup> Linda M. Dekkers,<sup>†</sup> Kristie Spijker,<sup>†</sup> E. W. Meijer,<sup>†</sup> Leo W. J. Klomp,<sup>‡</sup> and Maarten Merkx<sup>\*†</sup>

Contribution from the Laboratory of Macromolecular and Organic Chemistry, Department of Biomedical Engineering, Eindhoven University of Technology P.O. Box 513, 5600 MB Eindhoven, The Netherlands, and the Department of Metabolic and Endocrine Diseases, University Medical Centre Utrecht, Lundlaan 6, 3584 EA Utrecht, The Netherlands

Received February 11, 2006; E-mail: m.merkx@tue.nl

**Abstract:** The ability to image the concentration of transition metals in living cells in real time is important for further understanding of transition metal homeostasis and its involvement in diseases. The goal of this study was to develop a genetically encoded FRET-based sensor for copper(I) based on the copper-induced dimerization of two copper binding domains involved in human copper homeostasis, Atox1 and the fourth domain of ATP7B (WD4). A sensor has been constructed by linking these copper binding domains to donor and acceptor fluorescent protein domains. Energy transfer is observed in the presence of Cu(I), but the Cu(I)-bridged complex is easily disrupted by low molecular weight thiols such as DTT and glutathione. To our surprise, energy transfer is also observed in the presence of very low concentrations of Zn(II) ( $10^{-10}$  M), even in the presence of DTT. Zn(II) is able to form a stable complex by binding to the cysteines present in the conserved MXCXXC motif of the two copper binding domains. Co(II), Cd(II), and Pb(II) also induce an increase in FRET, but other, physiologically relevant metals are not able to mediate an interaction. The Zn(II) binding properties have been tuned by mutation of the copper-binding motif to the zinc-binding consensus sequence MDCXXC found in the zinc transporter ZntA. The present system allows the molecular mechanism of copper and zinc homeostasis to be studied under carefully controlled conditions in solution. It also provides an attractive platform for the further development of genetically encoded FRET-based sensors for Zn(II) and other transition metal ions.

### Introduction

Transition metals pose an interesting paradox to life since these metals are both essential as cofactors in many proteins and toxic in their free, aquated form. Research in the past decade, in particular on copper, has shown that transition metal homeostasis is a tightly regulated process in which the acquisition, distribution, and excretion of metals is controlled by specific proteins, resulting in very low free metal concentrations in cells.<sup>1</sup> The free copper concentration in the yeast cytoplasm has been estimated to be less than  $10^{-18}$  M,<sup>2</sup> and the transcriptional activator CueR from *E. coli* binds Cu(I) with an extremely low  $K_d$  of  $2 \times 10^{-21}$  M.<sup>3</sup> Under these conditions specific copper chaperone proteins are required to distribute this metal to different cellular targets.<sup>4,5</sup> In humans, copper targeted for excretion and incorporation into extracellular copper proteins is delivered by the copper chaperone protein Atox1 to copper-

transporting P-type ATPases (ATP7A and ATP7B) located in the Golgi membrane. Mutations in ATP7A and ATP7B result in copper depletion (Menkes Disease (MD)) or copper accumulation (Wilson's Disease (WD)), respectively.<sup>6</sup> All copper chaperones contain a conserved MXCXXC copper-binding motif, and homologous domains are also present at the intracellular N-terminus of ATP7A/B (six domains). This MXCXXC motif is arranged in a  $\beta\alpha\beta\beta\alpha\beta$  fold in which the two cysteines coordinate Cu(I) in either a two-coordinate, linear fashion<sup>7,8</sup> or in a three-coordinate complex with the third ligand being another amino acid or low molecular weight thiol.<sup>9–15</sup> This low coordination number is believed to favor Cu(I) and inhibit

<sup>†</sup> Eindhoven University of Technology.

<sup>‡</sup> University Medical Centre Utrecht.

- (1) Finney, L. A.; O'Halloran, T. V. *Science* **2003**, *300*, 931–936.
- (2) Rae, T. D.; Schmidt, P. J.; Pufahl, R. A.; Culotta, V. C.; O'Halloran, T. V. *Science* **1999**, *284*, 805–808.
- (3) Changela, A.; Chen, K.; Xue, Y.; Holschen, J.; Outten, C. E.; O'Halloran, T. V.; Mondragon, A. *Science* **2003**, *301*, 1383–1387.
- (4) O'Halloran, T. V.; Culotta, V. C. *J. Biol. Chem.* **2000**, *275*, 25057–25060.
- (5) Huffman, D. L.; O'Halloran, T. V. *Annu. Rev. Biochem.* **2001**, *70*, 677–701.

- (6) Schaefer, M.; Gitlin, J. D. *Am. J. Physiol.* **1999**, *276*, G311–314.
- (7) Wernimont, A. K.; Huffman, D. L.; Lamb, A. L.; O'Halloran, T. V.; Rosenzweig, A. C. *Nat. Struct. Biol.* **2000**, *7*, 766–771.
- (8) Rosenzweig, A. C.; Huffman, D. L.; Hou, M. Y.; Wernimont, A. K.; Pufahl, R. A.; O'Halloran, T. V. *Structure Fold Des.* **1999**, *7*, 605–617.
- (9) Pufahl, R. A.; Singer, C. P.; Peariso, K. L.; Lin, S. J.; Schmidt, P. J.; Fahrni, C. J.; Culotta, V. C.; Penner-Hahn, J. E.; O'Halloran, T. V. *Science* **1997**, *278*, 853–856.
- (10) Cobine, P. A.; George, G. N.; Jones, C. E.; Wickramasinghe, W. A.; Solioz, M.; Dameron, C. T. *Biochemistry* **2002**, *41*, 5822–5829.
- (11) Ralle, M.; Lutsenko, S.; Blackburn, N. J. *J. Biol. Chem.* **2003**, *278*, 23163–21170.
- (12) Arnesano, F.; Banci, L.; Bertini, I.; Huffman, D. L.; O'Halloran, T. V. *Biochemistry* **2001**, *40*, 1528–1539.
- (13) Anastassopoulou, J.; Banci, L.; Bertini, I.; Cantini, F.; Katsari, E.; Rosato, A. *Biochemistry* **2004**, *43*, 13046–13053.
- (14) Cobine, P. A.; George, G. N.; Winzor, D. J.; Harrison, M. D.; Moghaddas, S.; Dameron, C. T. *Biochemistry* **2000**, *39*, 6857–6863.

oxidation to Cu(II). The X-ray structure of Atox1 in the presence of Cu(I) revealed a second binding mode in which one copper ion is coordinated by cysteines from two Atox1 proteins in a three- or four-coordinate complex.<sup>7</sup> The latter structure is believed to represent the complex formed when copper is transferred from Atox1 to one of the copper binding domains of ATP7B.<sup>12,16</sup>

Zinc is well-known as a cofactor in numerous enzymes involved in hydrolysis and group transfer reactions,<sup>17</sup> but zinc also provides structural stability to proteins (e.g., in transcription factors),<sup>18,19</sup> and it has been implicated as a signaling molecule in neurotransmission.<sup>20</sup> Although its redox stability makes zinc less toxic than copper, free Zn(II) is known to interfere with many biological processes and is therefore probably maintained at low free concentrations as well.<sup>21–23</sup> Disruption of zinc homeostasis after ischemia or seizures and following head injury has been shown to result in an increase in free Zn(II) leading to neuronal damage,<sup>24–30</sup> whereas zinc deficiency resulting from defective zinc uptake leads to acrodermatitis enteropathica.<sup>31</sup> Although less is known about the molecular mechanism of cellular zinc homeostasis, some of the proteins involved may be homologous to proteins involved in copper homeostasis.<sup>32</sup> The cysteine-rich metallothioneins are known to bind both copper and zinc, for example.<sup>33,34</sup> Moreover, the Zn(II)-specific transporter ZntA from *E. coli* contains an MDCXXC motif in which Zn(II) is coordinated by both cysteines, the aspartic acid and a solvent molecule.<sup>35,36</sup> This raises the interesting question of how these similar metal binding sites distinguish between various transition metal ions.

An important prerequisite for further understanding of the mechanism of transition metal homeostasis and its involvement in diseases is the ability to image the concentration of transition metals in living cells in real time. Fluorescence microscopy is

ideally suited for this purpose, and the development of fluorescent probes that bind transition metal ions with high affinity and selectivity has recently become an area of active research.<sup>37–40</sup> A variety of Zn(II)-specific fluorescent dyes have been developed,<sup>41–59</sup> and recently the first two examples of Cu(I)-specific fluorescent chemosensors were reported.<sup>60,61</sup> Although several of these chemosensors have already been applied for intracellular imaging,<sup>62–64</sup> it has proven challenging to develop small molecule sensors with physiologically relevant binding constants. To improve the affinity and selectivity of metal binding, several groups have developed fluorescent sensors based on natural metal binding proteins. The Cu(I)-induced binding of the copper transcription activator CueR to a fluorescently labeled oligonucleotide has been used to detect nanomolar levels of Cu(I), but this sensor is unsuitable for intracellular imaging.<sup>65</sup> Protein-based fluorescent Zn(II) sensors include fluorescently labeled peptides based on Zn-finger domains,<sup>54,66,67</sup> carbonic anhydrase in combination with a Zn(II)-specific fluorescent substrate analogue,<sup>23,68,69</sup> and green fluorescent protein (GFP) variants with Zn(II) binding sites

- (15) Banci, L.; Bertini, I.; Del Conte, R.; Mangani, S.; Meyer-Klaucke, W. *Biochemistry* **2003**, *42*, 2467–2474.
- (16) Amesano, F.; Banci, L.; Bertini, I.; Cantini, F.; Ciofi-Baffoni, S.; Huffman, D. L.; O'Halloran, T. V. *J. Biol. Chem.* **2001**, *276*, 41365–41376.
- (17) Lipscomb, W. N.; Sträter, N. *Chem. Rev.* **1996**, *96*, 2375–2433.
- (18) Laity, J. H.; Lee, B. M.; Wright, P. E. *Curr. Opin. Struct. Biol.* **2001**, *11*, 39–46.
- (19) Berg, J. M.; Shi, Y. *Science* **1996**, *271*, 1081–1085.
- (20) Mocchegiani, E.; Bertoni-Freddari, C.; Marcellini, F.; Malavolta, M. *Prog. Neurobiol. (Amsterdam, Neth.)* **2005**, *75*, 367–390.
- (21) Outten, C. E.; O'Halloran, T. V. *Science* **2001**, *292*, 2488–2492.
- (22) Hitomi, Y.; Outten, C. E.; O'Halloran, T. V. *J. Am. Chem. Soc.* **2001**, *123*, 8614–8615.
- (23) Bozym, R. A.; Thompson, R. B.; Stoddard, A. K.; Fierke, C. A. *ACS Chem. Biol.* **2006**, *1*, 103–111.
- (24) Canzoniero, L. M.; Turetsky, D. M.; Choi, D. W. *J. Neurosci.* **1999**, *19*, RC31.
- (25) Sheline, C. T.; Behrens, M. M.; Choi, D. W. *J. Neurosci.* **2000**, *20*, 3139–3146.
- (26) Kim, Y. H.; Kim, E. Y.; Gwag, B. J.; Sohn, S.; Koh, J. Y. *Neuroscience* **1999**, *89*, 175–182.
- (27) Noh, K. M.; Koh, J. Y. *J. Neurosci.* **2000**, *20*, RC111.
- (28) Weiss, J. H.; Sensi, S. L.; Koh, J. Y. *Trends Pharmacol. Sci.* **2000**, *21*, 395–401.
- (29) Tonder, N.; Johansen, F. F.; Frederickson, C. J.; Zimmer, J.; Diemer, N. H. *Neurosci. Lett.* **1990**, *109*, 247–252.
- (30) Koh, J. Y.; Suh, S. W.; Gwag, B. J.; He, Y. Y.; Hsu, C. Y.; Choi, D. W. *Science* **1996**, *272*, 1013–1016.
- (31) Kury, S.; Dreno, B.; Bezieau, S.; Giraudet, S.; Kharfi, M.; Kamoun, R.; Mosain, J. P. *Nat. Genet.* **2002**, *31*, 239–240.
- (32) Amesano, F.; Banci, L.; Bertini, I.; Ciofi-Baffoni, S.; Molteni, E.; Huffman, D. L.; O'Halloran, T. V. *Genome Res.* **2002**, *12*, 255–271.
- (33) Vašák, M.; Hasler, D. W. *Curr. Opin. Chem. Biol.* **2000**, *4*, 177–183.
- (34) Calderone, V.; Dolderer, B.; Hartmann, H.-J.; Echner, H.; Luchinat, C.; Del Bianco, C.; Mangani, S.; Weser, U. *Proc. Natl. Acad. Sci. U.S.A.* **2005**, *102*, 51–56.
- (35) Banci, L.; Bertini, I.; Ciofi-Baffoni, S.; Finney, L. A.; Outten, C. E.; O'Halloran, T. V. *J. Mol. Biol.* **2002**, *323*, 883–897.
- (36) Rensing, C.; Mitra, B.; Rosen, B. P. *Proc. Natl. Acad. Sci. U.S.A.* **1997**, *94*, 14326–14331.
- (37) Jiang, P.; Guo, Z. *Coord. Chem. Rev.* **2004**, *248*, 205–229.
- (38) Kikuchi, K.; Komatsu, K.; Nagano, T. *Curr. Opin. Chem. Biol.* **2004**, *8*, 182–191.
- (39) Lim, N. C.; Freake, H. C.; Bruckner, C. *Chemistry* **2004**, *11*, 38–49.
- (40) Thompson, R. B. *Curr. Opin. Chem. Biol.* **2005**, *9*, 526–532.
- (41) Chang, C. J.; Nolan, E. M.; Jaworski, J.; Burdette, S. C.; Sheng, M.; Lippard, S. J. *Chem. Biol.* **2004**, *11*, 203–210.
- (42) Burdette, S. C.; Frederickson, C. J.; Bu, W.; Lippard, S. J. *J. Am. Chem. Soc.* **2003**, *125*, 1778–1787.
- (43) Burdette, S. C.; Walkup, G. K.; Spingler, B.; Tsien, R. Y.; Lippard, S. J. *J. Am. Chem. Soc.* **2001**, *123*, 7831–7841.
- (44) Chang, C. J.; Nolan, E. M.; Jaworski, J.; Okamoto, K.; Hayashi, Y.; Sheng, M.; Lippard, S. J. *Inorg. Chem.* **2004**, *43*, 6774–6779.
- (45) Gee, K. R.; Zhou, Z. L.; Qian, W. J.; Kennedy, R. J. *Am. Chem. Soc.* **2002**, *124*, 776–778.
- (46) Hanaoka, K.; Kikuchi, K.; Kojima, H.; Urano, Y.; Nagano, T. *Angew. Chem., Int. Ed.* **2003**, *42*, 2996–2999.
- (47) Hanaoka, K.; Kikuchi, K.; Kojima, H.; Urano, Y.; Nagano, T. *J. Am. Chem. Soc.* **2004**, *126*, 12470–12476.
- (48) Hirano, T.; Kikuchi, K.; Urano, Y.; Nagano, T. *J. Am. Chem. Soc.* **2002**, *124*, 6555–6562.
- (49) Kawabata, E.; Kikuchi, K.; Urano, Y.; Kojima, H.; Odani, A.; Nagano, T. *J. Am. Chem. Soc.* **2005**, *127*, 818–819.
- (50) Komatsu, K.; Kikuchi, K.; Kojima, H.; Urano, Y.; Nagano, T. *J. Am. Chem. Soc.* **2005**, *127*, 10197–10204.
- (51) Lim, N. C.; Yao, L.; Freake, H. C.; Bruckner, C. *Bioorg. Med. Chem. Lett.* **2003**, *13*, 2251–2254.
- (52) Maruyama, S.; Kikuchi, K.; Hirano, T.; Urano, Y.; Nagano, T. *J. Am. Chem. Soc.* **2002**, *124*, 10650–10651.
- (53) Nolan, E. M.; Lippard, S. J. *Inorg. Chem.* **2004**, *43*, 8310–8317.
- (54) Shultz, M. D.; Pearce, D. A.; Imperiali, B. *J. Am. Chem. Soc.* **2003**, *125*, 10591–10597.
- (55) Taki, M.; Wolford, J. L.; O'Halloran, T. V. *J. Am. Chem. Soc.* **2004**, *126*, 712–713.
- (56) Walkup, G. K.; Burdette, S. C.; Lippard, S. J.; Tsien, R. Y. *J. Am. Chem. Soc.* **2000**, *122*, 5644–5645.
- (57) Woodroffe, C. C.; Won, A. C.; Lippard, S. J. *Inorg. Chem.* **2005**, *44*, 3112–3120.
- (58) Woodroffe, C. C.; Lippard, S. J. *J. Am. Chem. Soc.* **2003**, *125*, 11458–11459.
- (59) Woodroffe, C. C.; Masalha, R.; Barnes, K. R.; Frederickson, C. J.; Lippard, S. J. *Chem. Biol.* **2004**, *11*, 1659–1666.
- (60) Yang, L.; McRae, R.; Henary, M. M.; Patel, R.; Lai, B.; Vogt, S.; Fahrni, C. J. *Proc. Natl. Acad. Sci. U.S.A.* **2005**, *102*, 11179–11184.
- (61) Zeng, L.; Miller, E. W.; Pralle, A.; Isacoff, E. Y.; Chang, C. J. *J. Am. Chem. Soc.* **2006**, *128*, 10–11.
- (62) Sensi, S. L.; Ton-That, D.; Sullivan, P. G.; Jonas, E. A.; Gee, K. R.; Kaczmarek, L. K.; Weiss, J. H. *Proc. Natl. Acad. Sci. U.S.A.* **2003**, *100*, 6157–6162.
- (63) Ueno, S.; Tsukamoto, M.; Hirano, T.; Kikuchi, K.; Yamada, M. K.; Nishiyama, N.; Nagano, T.; Matsuki, N.; Ikegaya, Y. *J. Cell Biol.* **2002**, *158*, 215–220.
- (64) Chang, C. J.; Jaworski, J.; Nolan, E. M.; Sheng, M.; Lippard, S. J. *Proc. Natl. Acad. Sci. U.S.A.* **2004**, *101*, 1129–1134.
- (65) Chen, P.; He, C. J. *Am. Chem. Soc.* **2004**, *126*, 728–729.
- (66) Godwin, H. A.; Berg, J. M. *J. Am. Chem. Soc.* **1996**, *118*, 6514–6515.
- (67) Walkup, G. K.; Imperiali, B. *J. Am. Chem. Soc.* **1996**, *118*, 3053–3054.
- (68) Thompson, R. B.; Maliwal, B. P.; Fierke, C. A. *Anal. Chem.* **1998**, *70*, 1749–1754.
- (69) Thompson, R. B.; Cramer, M. L.; Bozym, R. J. *Biomed. Opt.* **2002**, *7*, 555–560.

introduced by protein engineering.<sup>70,71</sup> The latter have the important advantage of being genetically encoded (i.e., no synthetic fluorescent groups are used), but the present GFP-based Zn(II) sensors show only weak-to-moderate affinity for Zn(II) ( $K_d = 50\text{--}700\ \mu\text{M}$ ).

Fluorescence resonance energy transfer (FRET) between donor and acceptor fluorescent protein domains is an effective way to translate conformational changes in a sensor domain into a ratiometric fluorescent signal. Tsien and co-workers pioneered this concept by constructing the calcium sensor Cameleon in which the calcium binding protein calmodulin was fused to two spectral variants of GFP.<sup>72</sup> Calcium binding to calmodulin induces a conformational change in these fusion proteins that brings the donor and acceptor domains closer together which results in increased FRET. Unlike synthetic fluorescent probes which need to be introduced inside the cell via microinjection or passive diffusion, genetically encoded sensors such as Cameleon consist entirely of amino acids and can be produced inside cells after transfection of their corresponding genes. Attachment of signal sequences and regulation of transcription also allow control over their subcellular localization and concentration. Using yeast two-hybrid analysis, we and others previously observed copper-dependent interactions between copper chaperone proteins and copper binding domains present in their physiological target proteins.<sup>73–75</sup> The strongest interaction was observed between Atox1 and the fourth copper binding domain of Wilson's disease protein, WD4.<sup>75</sup> The goal of the work presented here was to develop a genetically encoded FRET-based sensor for Cu(I) using the Cu(I)-induced complex formation between these two protein domains (Figure 1). Not only the Cu(I) binding properties of the system are reported but also its surprisingly high affinity for Zn(II). The implications of our findings for the understanding of the coordination chemistry of metallochaperones and the development of genetically encoded sensors for zinc imaging are discussed.

## Materials and Methods

**General.** All restriction enzymes were obtained from New England Biolabs. Oligonucleotides were purchased from MWG Biotech, and DNA sequencing was performed by BaseClear.

**Plasmid Constructs.** The plasmids encoding for His-tagged CFP-WD4 and CFP-Atox1 fusion proteins were constructed in two steps. First, the copper binding domains Atox1 or WD4 (the fourth domain of ATP7B, aa 355–426) were amplified by PCR from human liver cDNA using specific oligonucleotides containing either a *BspE* I (5'-GCA TCC GGA ATG CCG AAG CAC GAG TTC-3' for Atox1 and 5'-GCA TCC GGA CAG GGC ACA TGC AGT ACC-3' for WD4) or an *Xho* I restriction site (underlined) (5'-GCT CTC GAG CTC AAG GCC AAG GTA G-3' for Atox1 and 5'-CGT CTC GAG GAC TGA AGC CTC AAA TCC C-3' for WD4) added to their 5' ends. The PCR fragments were TA cloned in pCR2.1 (Invitrogen), digested with *BspE* I and *Xho* I, and ligated into pECFP-C1 (Clontech), which was

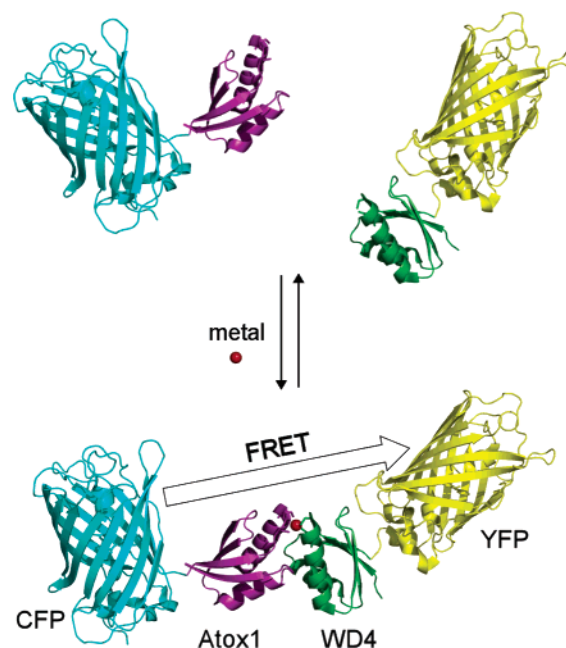


**Figure 1.** Design of a ratiometric, fluorescent sensor based on the copper binding proteins Atox1 and WD4. In the presence of the metal, a metal-bridged Atox1-WD4 dimer is formed, which can be detected through FRET between donor (CFP: cyan fluorescent protein) and acceptor (YFP: yellow fluorescent protein) domains linked to Atox1 and WD4, respectively.

predigested with *BspE* I and *Xho* I. In the second step, the CFP-Atox1 and CFP-WD4 fragments were amplified by PCR using primers that add an *Nde* I restriction site (5'-GCT AGC ATA TGG TGA GCA AGG GCG AG-3' for both constructs) and an *Not* I restriction site and a stop codon (5'-CTA AAG CGG CCG CTC ACT CAA GGC CAA GGT AG-3' for CFP-Atox1 and 5'-CTA AAG CGG CCG CTC AGA CTG AAG CCT CAA ATC C-3' for CFP-WD4). After digestion with *Nde* I and *Not* I, the PCR fragments were ligated into the *Nde* I and *Not* I sites of pET28-a (Novagen), yielding pET28-CFP-Atox1 and pET28-CFP-WD4.

The plasmids encoding Atox1-YFP and WD4-YFP were constructed in a similar manner. The copper binding domains Atox1 or WD4 were amplified by PCR from human liver cDNA using specific oligonucleotides containing either an *Sac* II (5'-GCA CCG CGG ATG CCG AAG CAC GAG TTC TC-3' for Atox1 and 5'-GCA CCG CGG ATG CAG GGC ACA TGC AGT ACC-3' for WD4) or a *Bam*HI restriction site (5'-CGT GGA TCC GAC TCA AGG CCA AGG TAG G-3' for Atox1 and 5'-CGT GGA TCC GAG ACT GAA GCC TCA AAT CCC-3' for WD4) added to their 5' ends. The PCR fragments were TA cloned in pCR2.1 (Invitrogen), digested with *Sac* II and *Bam*HI, and ligated into pEYFP-N1 (Clontech), which was predigested with *Sac* II and *Bam*HI. In the second step, the Atox1-YFP and WD4-YFP fragments were amplified by PCR using primers that add an *Nde* I restriction site (5'-GCT AGC ATA TGC CGA AGC ACG AGT TCT C-3' for Atox1-YFP and 5'-GCT AGC ATA TGC AGG GCA CAT GCA GTA CC-3' for WD4-YFP) and an *Not* I restriction site and a stop codon (5'-GGT ATG GCT GAT TAT GAT CTA GAG TCG-3' for both constructs). After digestion with *Nde* I and *Not* I, the PCR fragments were ligated into the *Nde* I and *Not* I sites of pET28-a (Novagen), yielding pET28-Atox1-YFP and pET28-WD4-YFP.

Site-directed mutagenesis was done using the Stratagene QuikChange kit according to the instructions of the manufacturer. The following primers were used: CFP-Atox1-T252D, 5'-CGA GTT CTC TGT GGA CAT GGA CTG TGG AGG CTG TGC TGA AGC-3'; WD4-YFP-T16D, 5'-GCC ATT GCC GGC ATG GAC TGT GCA TCC TGT GTC C-3'; CFP-Atox1-C253S/C256S, 5'-CTC TGT GGA CAT GAC CAG TGG AGG CAG TGC TGA AGC TGT CTC-3'; WD4-YFP-C17S/

(70) Barondeau, D. P.; Kassmann, C. J.; Tainer, J. A.; Getzoff, E. D. *J. Am. Chem. Soc.* **2002**, *124*, 3522–3524.

(71) Jensen, K. K.; Martini, L.; Schwartz, T. W. *Biochemistry* **2001**, *40*, 938–945.

(72) Miyawaki, A.; Llopis, J.; Heim, R.; McCaffery, J. M.; Adams, J. A.; Ikura, M.; Tsien, R. Y. *Nature* **1997**, *388*, 882–887.

(73) Lin, S. J.; Pufahl, R. A.; Dancis, A.; O'Halloran, T. V.; Culotta, V. C. *J. Biol. Chem.* **1997**, *272*, 9215–9220.

(74) Larin, D.; Mekios, C.; Das, K.; Ross, B.; Yang, A. S.; Gilliam, T. C. *J. Biol. Chem.* **1999**, *274*, 28497–28504.

(75) van Dongen, E. M.; Klomp, L. W.; Merks, M. *Biochem. Biophys. Res. Commun.* **2004**, *323*, 789–795.



C20S, 5'-CCA TTG CCG GCA TGA CCA GTG CAT CCA GTG TCC ATT CCA TTG-3'. DNA sequencing confirmed the correct sequences of these mutants.

**Protein Production.** The pET28 expression plasmids encoding CFP-WD4, CFP-Atox1, WD4-YFP, and Atox1-YFP were transformed into chemically competent *E. coli* BL21(DE3) according to the manufacturer's instructions (Novagen). Bacteria were grown in LB medium containing 30  $\mu$ g/mL kanamycin at 225 rpm and 37 °C to an optical density between 0.6 and 1 at 600 nm. Expression was induced with 0.1 mM IPTG, and bacteria were grown for another 4 h at 37 °C. After centrifugation at 10 000 g at 4 °C for 20 min, the cell pellet was resuspended according to the BugBuster protocol (Novagen) and incubated on a shaking platform for 20 min at room temperature. The soluble fraction was separated from the insoluble fraction by centrifugation at 40 000 g for 20 min at 4 °C. The fusion proteins were purified from the soluble protein fraction using HisBind nickel affinity chromatography according to the manufacturer's instructions (Novagen). The His-tag was removed by digestion with thrombin (Novagen) (0.2 U/mL; protein concentration of 0.2 mg/mL) for 8–24 h at 4 °C. The fusion proteins were separated from the His-tag by size exclusion chromatography (SEC) using an S200 Sephacryl column. SDS-PAGE analysis and ESI-MS results both confirmed the cleavage of the His-tag from the proteins and the correct molecular weight. The copper content was determined using a BCA assay<sup>76</sup> that was calibrated using a copper ICP standard (Merck).

**Fluorescence Experiments.** Fluorescence spectra were recorded on a Perkin-Elmer LS 50B luminescence spectrometer. Unless stated otherwise, spectra were measured using 2  $\mu$ M of each fusion protein in 50 mM Tris, 100 mM NaCl, 10% glycerol pH 7.5 using an excitation wavelength of 420 nm. The concentration of fusion proteins was quantified using  $A_{435}$  and a molar extinction coefficient of 32 500 M<sup>-1</sup> cm<sup>-1</sup> for CFP fusion proteins<sup>77</sup> and using  $A_{515}$  and a molar extinction coefficient of 84 000 M<sup>-1</sup> cm<sup>-1</sup> for YFP fusion proteins.<sup>78</sup> DTT (1 mM) or TCEP (0.5 mM) was used as a reducing agent to prevent oxidation of the cysteines in the metal binding motif under aerobic conditions. The YFP/CFP ratio is defined as the fluorescence intensity of the YFP fusion protein at 527 nm divided by the fluorescence intensity of the CFP fusion protein at 475 nm.

**Determination of Metal Selectivity.** To complex adventitious metals that are already present in the buffer, 15  $\mu$ M EDTA was first added to CFP-Atox1 and WD4-YFP (2  $\mu$ M each) in 50 mM Tris, 100 mM NaCl, 0.5 mM TCEP or 1 mM DTT, 10% glycerol pH 7.5. The indicated metals were added from 10 mM stock solutions to a final concentration of 20  $\mu$ M. Prior to and after metal addition, the fluorescence emission spectrum was recorded, and the YFP/CFP ratio was calculated. Stock solutions were made in water from ZnCl<sub>2</sub>, CoSO<sub>4</sub>, (NH<sub>4</sub>)<sub>2</sub>Fe(SO<sub>4</sub>)<sub>2</sub>, MgSO<sub>4</sub>, NiSO<sub>4</sub>, CaCl<sub>2</sub>, CuSO<sub>4</sub>, and Cd(OAc)<sub>2</sub>. Pb(II) was diluted from a 1000  $\mu$ g/mL lead atomic standard solution (Sigma).

**Copper Titrations.** All titrations using Cu(I) were done under carefully controlled anaerobic conditions. CFP-Atox1 and WD4-YFP in 50 mM Tris, 100 mM NaCl, pH 8 buffer were transferred into a Coy anaerobic chamber, incubated overnight with 2 mM DTT to completely reduce the metal-binding cysteines, and treated with 5 mM sodium dithionite (Sigma) for 5 min to remove traces of O<sub>2</sub>. Slide-alalyzer minidialysis units (Pierce) were used to dialyze the protein 3 times for at least 1 h against anaerobic buffer (50 mM Tris, 100 mM NaCl, pH 8) to remove DDT and sodium dithionite. The fusion proteins (2  $\mu$ M each) in 50 mM Tris, 100 mM NaCl, 10% glycerol pH 8 were transferred into a fluorescence cuvette sealed with a rubber septum and transferred out of the anaerobic chamber. A 25 mM Cu(I) stock solution was prepared by dissolving Cu(I)(CH<sub>3</sub>CN)<sub>4</sub>PF<sub>6</sub> (Sigma) in degassed 100% acetonitrile under anaerobic conditions. EDTA, Zn(II), and Cu-

(I) were added to the cuvette from anaerobic stock solutions using Hamilton gastight syringes.

**Zinc Titrations.** Zn(II) was titrated in either a buffering system consisting of 1 mM EGTA and 0.1–0.9 mM Zn(II) or a system consisting of 1 mM EDTA, 2 mM Ca(II), and 0.1–0.9 mM Zn(II). All titrations were done using 2  $\mu$ M CFP-Atox1 and 2  $\mu$ M WD4-YFP in 50 mM Tris, 100 mM NaCl, 10% glycerol pH 7.5 in a total volume of 500  $\mu$ L. For the EGTA buffering system, free Zn(II) concentrations were calculated using the MaxChelator program.<sup>79</sup> For the calcium–EDTA buffering system, free Zn(II) concentrations were calculated using the method described by Walkup.<sup>56</sup> After each Zn(II) addition, the fluorescence emission spectrum of the mixture was measured (excitation: 420 nm), and the percentage of the YFP/CFP ratio increase (indicating FRET) was calculated. The formation constant of the equilibrium among CFP-Atox1, WD4-YFP, and Zn(II) was determined using eq 1 and the nonlinear least-squares fit procedure of Origin 6.0, in which  $[\text{protein}]_{\text{total}} = [\text{CFP-Atox1}]_{\text{total}} = [\text{WD4-YFP}]_{\text{total}} = 2 \times 10^{-6}$  M.

$$[\text{complex}] = \left\{ 2[\text{protein}]_{\text{total}} + 1/(\beta[\text{Zn}^{2+}]_{\text{free}}) - \sqrt{(-2[\text{protein}]_{\text{total}} - 1/(\beta[\text{Zn}^{2+}]_{\text{free}}))^2 - 4[\text{protein}]_{\text{total}}^2} \right\} / 2 \quad (1)$$

## Results

Four fusion proteins were constructed in which Atox1 and WD4 were linked to either Cyan Fluorescent Protein (CFP) or Yellow Fluorescent Protein (YFP). The fusion proteins were cloned with an N-terminal His-tag in pET28 and overexpressed in *E. coli*. Purification using Ni-affinity chromatography and subsequent proteolytic removal of the His-tag resulted in the isolation of CFP-Atox1, CFP-WD4, Atox1-YFP, and WD4-YFP in good yields (~50–100 mg/L). All four fusion proteins showed the optical properties (absorption and emission spectra) characteristic of CFP and YFP, respectively, indicating proper folding of the fluorescent protein domain. Metal analysis showed less than 0.05 Cu/protein. To obtain evidence for Cu(I)-induced FRET, various 1:1 combinations of CFP and YFP fusion proteins were studied using fluorescence spectroscopy. Figure 2A shows the emission spectra of CFP-Atox1 and WD4-YFP when excited at 420 nm, and their summation. As expected at this excitation wavelength, a strong emission signal is observed for CFP-Atox1, and a weak signal, for WD4-YFP. Unexpectedly, the spectrum for the 1:1 mixture of CFP-Atox1 and WD4-YFP is not a simple summation of the emission spectra obtained for the separate proteins (Figure 2B). The emission peak at 475 nm is significantly decreased, and the emission at 527 nm is increased with respect to the summation, indicating that energy transfer between the two fusion proteins is taking place even in the absence of added Cu(I). Because the fusion proteins did not contain detectable amounts of copper and because the presence of trace amounts of Cu(I) in our buffers is highly unlikely, the interaction must be Cu(I)-independent. A similar but slightly smaller change in donor and acceptor emissions was observed for the reciprocal pair, CFP-WD4 and Atox1-YFP (see Supporting Information). FRET was not observed when CFP and YFP fusion proteins with the same copper binding domains were used (e.g., CFP-Atox1/Atox1-YFP), as the emission spectra completely overlapped with the summation of the emission spectra of the individual domains (see Supporting Information). This result is consistent with results from yeast two-hybrid analyses, in which the formation of homodimers was

(76) Brenner, A. J.; Harris, E. D. *Anal. Biochem.* **1995**, *226*, 80–84.

(77) Cubitt, A. B.; Woollenweber, L. A.; Heim, R. *Methods Cell Biol.* **1999**, *58*, 19–30.

(78) Patterson, G.; Day, R. N.; Piston, D. J. *Cell Sci.* **2001**, *114*, 837–838.

(79) Patton, C.; Thompson, S.; Epel, D. *Cell Calcium* **2004**, *35*, 427–431.

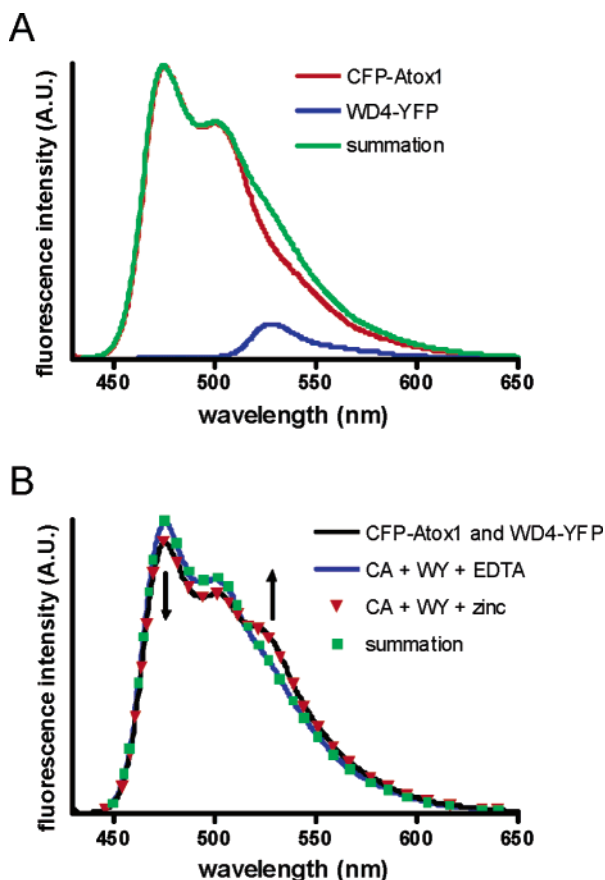


**Figure 2.** Emission spectra of CFP-Atox1 and WD4-YFP showing Zn(II)-dependent FRET. All spectra were measured in 50 mM Tris, 100 mM NaCl, 10% glycerol, 0.5 mM TCEP, pH 7.5 using protein concentrations of 2  $\mu$ M and 420 nm excitation. Panel A shows the emission spectra of CFP-Atox1 and YFP-WD4 when measured separately, and the summation of both spectra that is expected for a mixture of CFP-Atox1 and YFP-WD4 in the absence of FRET. Panel B shows the emission spectrum determined for a 1:1 mixture of CFP-Atox1 (CA) and WD4-YFP (WY) in normal buffer (black line), upon addition of 15  $\mu$ M EDTA (blue line), and after subsequent addition of 17  $\mu$ M Zn(II) (red triangle). The summation of the individually determined spectra of CFP-Atox1 and WD4-YFP is shown for comparison.

also not detected, and shows that the interaction between Atox1 and WD4 is specific. The observed decrease in donor emission corresponds to a donor–acceptor distance of  $\sim 75$  Å in the complex.<sup>80</sup> This distance is reasonable, given that the distance between the terminal residues in the Atox1-dimer is  $\sim 50$  Å and the distance between the chromophore and the terminal residues of CFP/YFP is at least 15 Å.<sup>7</sup>

The two cysteines present in the copper binding domains are strong metal binding ligands. To test whether the interaction observed between Atox1 and WD4 fusion proteins is mediated by metal ions other than copper, the effect of metal chelators was studied. Addition of 15  $\mu$ M EDTA to CFP-Atox1/WD4-YFP resulted in an emission spectrum that was indistinguishable from the calculated spectrum in the absence of FRET (Figure 2B), suggesting that the interaction was indeed metal-dependent. Similar results were obtained using 1,10-phenanthroline, another nonspecific metal chelator for divalent metal ions (not shown). Since Zn(II) is normally present at  $\sim 1$   $\mu$ M in buffers when no

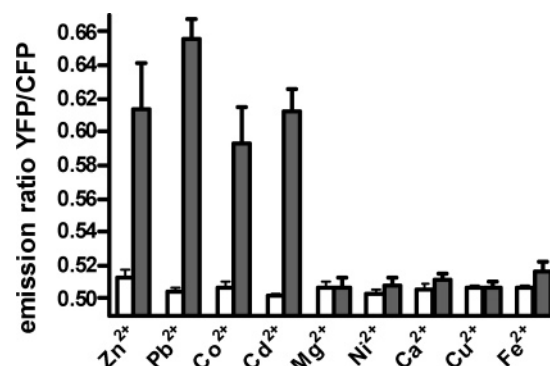


**Figure 3.** Metal dependency of the interaction between CFP-Atox1 and WD4-YFP. The YFP/CFP emission ratio was determined using 2  $\mu$ M CFP-Atox1, 2  $\mu$ M WD4-YFP in 50 mM Tris, 100 mM NaCl, 0.5 mM TCEP, 10% glycerol, pH 7.5. White bars represent the ratio in the presence of 15  $\mu$ M EDTA, and the gray bars show the ratio after subsequent addition of 20  $\mu$ M of the indicated metal. The error bars represent the standard deviation determined from three independent experiments.

special precautions are taken,<sup>81</sup> we tested whether stepwise addition of low concentrations of Zn(II) could restore the interaction that was disrupted by 15  $\mu$ M EDTA. No change in fluorescence emission was observed up to a concentration of 13  $\mu$ M, but upon further addition of Zn(II) the YFP/CFP ratio increased to the same level as that before EDTA addition at 17  $\mu$ M Zn(II). Similar results were obtained for the reciprocal pair CFP-WD4/Atox1-YFP, but the spectra of CFP-WD4/WD4-YFP and CFP-Atox1/Atox1-YFP were not affected by addition of either EDTA or Zn(II) (see Supporting Information).

The unexpected Zn(II)-induced complex formation prompted us to investigate the metal selectivity of the interaction. CFP-Atox1 and WD4-YFP were first treated with 15  $\mu$ M EDTA to remove advantageous Zn(II), followed by an excess of a variety of divalent metal ions (Figure 3). Of all metals tested only Co(II), Cd(II), and Pb(II) showed a similar increase in FRET as observed with Zn(II). In the presence of 1 mM DTT (instead of TCEP), FRET was still observed for Zn(II), Co(II), and Cd(II) but not for Pb(II) (not shown). All of these metal ions are known to have a similar coordination chemistry as that of Zn(II). Co(II) and Cd(II) are often used as spectroscopic probes for Zn(II) binding sites,<sup>81</sup> whereas Pb(II) is known to bind to cysteine-rich Zn(II) binding sites.<sup>82–84</sup>

Binding studies with Cu(I) are more complicated than those with the divalent metal ions described above. Although Cu(I) titrations were done under carefully controlled anaerobic conditions using freshly prepared anaerobic stock solutions of Cu(I)(CH<sub>3</sub>CN)<sub>4</sub>–PF<sub>6</sub> in CH<sub>3</sub>CN, we initially did not observe Cu(I)-induced FRET. We eventually did observe Cu(I)-induced FRET, but only after extensive dialysis of the proteins to completely remove DTT. Figure 4 shows an experiment in which CFP-Atox1 and WD4-YFP were mixed at a 1:1 ratio and transferred to an anaerobic cuvette. First 15  $\mu$ M EDTA was added to remove advantageous Zn(II) resulting in a decrease of the emission ratio from 0.60 to 0.54. Addition of 30  $\mu$ M Cu(I) resulted in a clear increase in the YFP/CFP ratio, providing

(81) Auld, D. S. *Methods Enzymol.* **1988**, 158, 71–79.

(82) Magyar, J. S.; Weng, T. C.; Stern, C. M.; Dye, D. F.; Rous, B. W.; Payne, J. C.; Bridgewater, B. M.; Mijovilovich, A.; Parkin, G.; Zaleski, J. M.; Penner-Hahn, J. E.; Godwin, H. A. *J. Am. Chem. Soc.* **2005**, 127, 9495–9505.

(83) Godwin, H. A. *Curr. Opin. Chem. Biol.* **2001**, 5, 223–227.

(84) Dudgey, T.; Lim, C. *Chem. Rev.* **2003**, 103, 773–787.

(80) The distance  $r$  was calculated using the Förster equation ( $E = R_0^6/(R_0^6 + r^6)$ ) with  $E = 1 - F_{DA}/F_D$  and  $R_0 = 49$  Å (Patterson, G. H.; Piston, D. W.; Barisas, B. G. *Anal. Biochem.* **2000**, 284, 438–440).

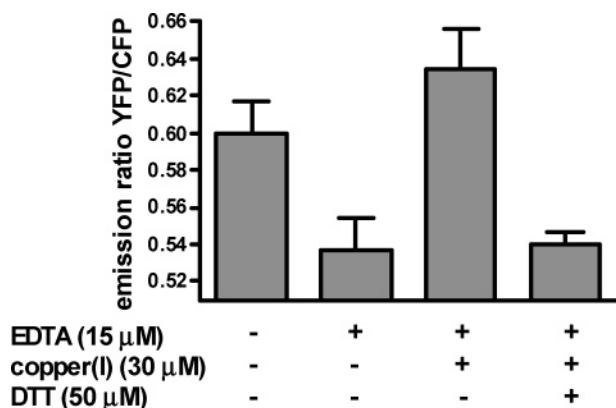


**Figure 4.** Cu(I) dependency of the interaction between CFP-Atox1 and WD4-YFP. The YFP/CFP emission ratios were determined using anaerobic samples of 2 μM CFP-Atox1, 2 μM WD4-YFP, 50 mM Tris, 100 mM NaCl, 10% glycerol, pH 8, followed by the subsequent anaerobic addition of 15 μM EDTA, 30 μM Cu(I), and 50 μM DTT. The error bars represent the standard deviation determined from three independent experiments.

strong evidence for the formation of a Cu(I)-bridged ternary complex. The interaction was readily disrupted upon addition of a low amount of DTT (50 μM), however. The same effect was observed in the presence of the same concentration of glutathione, showing that the interaction is highly sensitive to free thiols.

To test whether the copper binding domains would still bind Cu(I) in the presence of DTT, competition experiments between Zn(II) and Cu(I) were performed. In the first experiment, an anaerobic mixture of 2 μM CFP-Atox1 and 2 μM WD4-YFP was treated with 15 μM EDTA followed by 30 μM Cu(I) (Figure 5A). Addition of EDTA again resulted in disruption of the interaction, and no restoration of FRET was observed upon addition of Cu(I). Subsequent addition of 20 μM Zn(II) also did not lead to a change in the YFP/CFP ratio, however, suggesting that copper binding to the metal binding sites prevented the Zn(II)-mediated dimerization. A titration experiment in which the apo proteins were preincubated with different amounts of Cu(I) showed that Zn(II) binding is already completely blocked after addition of 1 equiv (4 μM) of Cu(I) (Figure S4), showing that Cu(I) binds significantly stronger than Zn(II). In a second experiment, the Zn(II)-bridged complex was first formed by addition of 20 μM Zn(II) to CFP-Atox1 and WD4-YFP (Figure 5B). A clear decrease in the YFP/CFP ratio was observed after anaerobic addition of Cu(I) (30 μM) to this sample, again showing that Cu(I) binds stronger than Zn(II). Based on these experiments we conclude that the copper binding domains present in CFP-Atox1 and WD4-YFP strongly bind Cu(I) also in the presence of DTT but that the Cu(I)-bridged dimer is not formed under these conditions.

Although in principle a sensitive ratiometric fluorescent sensor for Cu(I) was obtained, the thiol sensitivity of the sensor presents a major problem for practical application of this sensor. In contrast, the CFP-Atox1/WD4-YFP combination does constitute an attractive ratiometric Zn(II) sensor with surprisingly high Zn(II) affinity even in the presence of DTT. Obviously, the sensor would not work in the presence of large amounts of Cu(I), but Figure 3 shows that it is specific compared to most other physiologically relevant divalent metal ions. To establish its usefulness as a biological Zn(II) sensor, titration experiments were performed using metal buffers that allow control of free

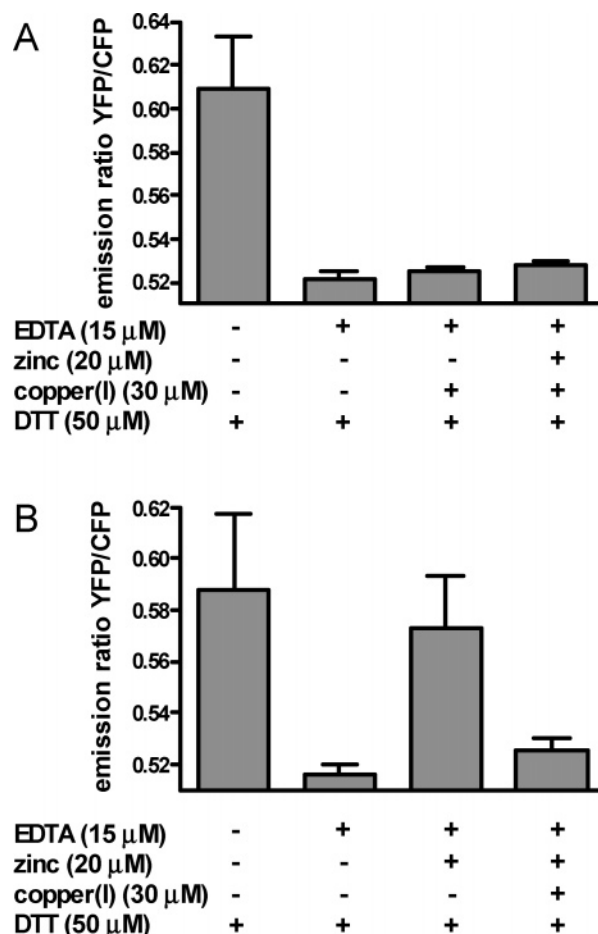


**Figure 5.** Experiments showing competition between Zn(II) and Cu(I) binding. All experiments were done using anaerobic samples containing 2 μM CFP-Atox1, 2 μM WD4-YFP, 50 mM Tris, 100 mM NaCl, 50 μM DTT, 10% glycerol, pH 8. (Panel A) YFP/CFP emission ratio after subsequent addition of 15 μM EDTA, 30 μM Cu(I), and finally 20 μM Zn(II). (Panel B) YFP/CFP emission ratio after subsequent addition of 15 μM EDTA, 20 μM Zn(II), and 30 μM Cu(I).

Zn(II) concentrations in the picomolar to nanomolar range. Two different metal buffer systems were used, EDTA/Ca(II)/Zn(II) and EGTA/Zn(II) to minimize the chance of making systematic errors in calculating free Zn(II) concentrations. Figure 6A shows that the increase of the YFP/CFP ratio is half-maximal at ~350 pM free Zn(II) at pH 7.5. A nonlinear fit of the EGTA/Zn(II) titration curve using the equation describing the formation of a ternary complex of CFP-Atox1–Zn(II)–WD4-YFP yields an apparent formation constant of  $4.5 \times 10^{15} \text{ mol}^{-2} \text{ L}^2$ .

To obtain unambiguous evidence that Zn(II) is mediating complex formation by binding to the two cysteines of each copper-binding domain, mutant proteins were made of both CFP-Atox1 and WD4-YFP in which both of the cysteines in the MXCXXC motif were replaced by serines. As expected, Zn(II) titration to these Cys-to-Ser mutant proteins did not show any evidence for complex formation, as the emission ratio was unaffected (Figure 6B). In an attempt to increase the Zn(II) affinity of the sensor even further, mutants of CFP-Atox1 and WD4-YFP were constructed in which the threonine (T) present in the MTCXXC motif was replaced by an aspartic acid (D). The rationale behind this mutation was that an MDCXXC motif is found in the Zn(II)-specific metal transport ATPase ZntA. The presence of the negatively charged aspartic acid is thought



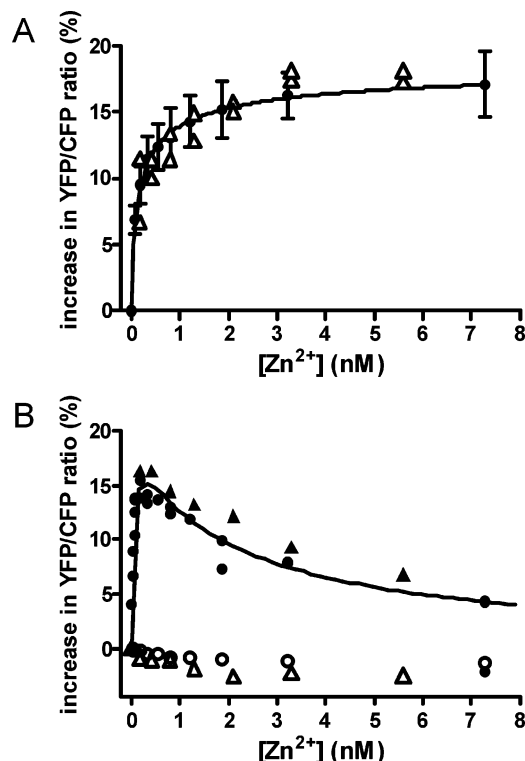


**Figure 6.** Zn(II) titration experiments for “wild-type” CFP-Atox1/WD4-YFP (panel A) and for variants with mutations in the metal binding site (panel B). All titrations were done using 2  $\mu$ M concentrations of each protein in 50 mM Tris, 100 mM NaCl, 0.5 mM TCEP, 10% glycerol, pH 7.5, using either EDTA (1 mM EDTA, 2 mM CaCl<sub>2</sub>; triangles) or EGTA (1 mM EGTA; circles) metal buffering systems. (Panel A) Zinc titration to CFP-Atox1 and WD4-YFP. The solid line is a fit of the data obtained using the EGTA buffering system (three independent experiments) using the equation for the formation of a ternary CFP-Atox1–Zn(II)–WD4-YFP complex ( $\beta = 4.5 \times 10^{15} \text{ mol}^{-2} \text{ L}^2$ ). (Panel B) Zinc titrations for the combination of CFP-Atox1-C253S/C256S and WD4-YFP-C16S/C20S (open symbols) and for the combination of CFP-Atox1-T252D and WD4-YFP-T16D (closed symbols).

to increase the affinity of these metal sites for divalent metal ions over monovalent metal ions such as Cu(I). Interestingly, titration of Zn(II) to a 1:1 mixture of Thr-to-Asp mutants of CFP-Atox1 and WD4-YFP results in a rapid increase in FRET at low concentrations of Zn(II), followed by a decrease in FRET at higher Zn(II) concentrations (Figure 6B). Compared to the titration curve of the “wild-type” proteins, complex formation was reached at substantially lower Zn(II) concentrations. The disruption of the complex at higher Zn(II) concentrations is probably due to binding of a Zn(II) ion to each of the copper binding domains, which is enabled by the presence of an additional metal binding carboxylate group.

## Discussion

Our sensor design was based on several observations that suggested that Cu(I)-bridged complexes can be formed between copper binding domains involved in cellular copper homeostasis. Yeast two-hybrid studies showed that interactions between copper binding domains can be disrupted by addition of the copper(I)-specific chelator bathocuproine disulfonic acid (BCS).<sup>74,85</sup> In fact, our choice for Atox1 and WD4 was based on a recent yeast two-hybrid study that showed a copper-specific

interaction between these domains that could be interrupted by addition of BCS or by addition of extra copper to the medium.<sup>75</sup> Very recently, NMR studies also showed a preference of Cu(I)-Atox1 for binding to the fourth domain of ATP7B.<sup>86</sup> The crystal structure of Atox1 in the presence of Cu(I) also shows a copper-bridged dimer in which the Cu(I) is bound to 3 or 4 cysteines from the copper binding motifs present in each monomer.<sup>7</sup> Other studies suggesting the presence of Cu(I)-mediated interactions between copper binding domains include surface plasmon resonance,<sup>87</sup> NMR,<sup>15,86</sup> gel filtration chromatography,<sup>88</sup> and intracellular detection of FRET between CFP and YFP fusion proteins of Atox1.<sup>89</sup> The generation of CFP/YFP fusion proteins reported here allows one to study the metal-mediated interaction under carefully controlled conditions in solution using FRET and, thus, provides an attractive alternative method to study the mechanism and metal selectivity of proteins involved in copper homeostasis. Although our results confirm the presence of a Cu(I)-bridged protein interaction between Atox1 and WD4, energy transfer was readily disrupted by the addition of relatively low concentrations of free thiols such as DTT and glutathione. The participation of an additional thiol group provides an extra coordinating group for Cu(I) besides the two cysteines of the copper-binding motif, resulting in a three-coordinated Cu(I) complex. Stabilization of the monomeric form by DTT and other exogenous ligands has been observed before in EXAFS and NMR studies.<sup>11,88,90</sup> Since intracellular protein concentrations are probably close to the protein concentrations used in our FRET experiments and because the intracellular glutathione concentration is  $\sim 5$  mM, our findings suggest that in vivo the Cu(I)-bridged complex between Atox1 and ATP7B is only formed transiently.

The thiol sensitivity of CFP-Atox1 and WD4-YFP limits the applicability and reliability of the Cu(I) sensor as the formation of a Cu(I)-bound monomer stabilized by glutathione will probably be favored over a Cu(I)-bridged dimer (Figure 7A). Zn(II) was shown to form a stable complex between CFP-Atox1 and WD4-YFP even in the presence of thiols, however (Figure 7B). Mutagenesis studies showed that the cysteines present in the MXCXXC motifs of the copper-binding domain are essential for this interaction. Complementary protein–protein interactions are also important, however, since Zn(II)-induced dimerization was not observed for the CFP-Atox1/Atox1-YFP or CFP-WD4/WD4-YFP pair. The most likely coordination mode of Zn(II) is a tetrahedral complex of four cysteines residues, which is well documented for structural zinc sites that are found in certain zinc finger domains present in hormone receptors and GATA proteins.<sup>84,91</sup> Zn(II) generally prefers a tetrahedral ligand geometry, although five- and six-coordination are also possible.<sup>84</sup> Low coordination numbers are not stable, however, which explains why Zn(II) prefers to form complexes with two MXCXXC sites. This preference of Zn(II) for coordination by

(85) Casareno, R. L.; Waggoner, D.; Gitlin, J. D. *J. Biol. Chem.* **1998**, *273*, 23625–23628.

(86) Achila, D.; Banci, L.; Bertini, I.; Bunce, J.; Ciofi-Baffoni, S.; Huffman, D. L. *Proc. Natl. Acad. Sci. U.S.A.* **2006**, *103*, 5729–5734.  
 (87) Strausak, D.; Howie, M. K.; Firth, S. D.; Schlicksupp, A.; Pipkorn, R.; Multhaup, G.; Mercer, J. F. *J. Biol. Chem.* **2003**, *278*, 20821–20827.  
 (88) Kihlken, M. A.; Leech, A. P.; Le Brun, N. E. *Biochem. J.* **2002**, *368*, 729–739.  
 (89) Tanchou, V.; Gas, F.; Urvoas, A.; Cougouluegne, F.; Ruat, S.; Averseng, O.; Quemeneur, E. *Biochem. Biophys. Res. Commun.* **2004**, *325*, 388–394.  
 (90) Banci, L.; Bertini, I.; Del Conte, R.; Markey, J.; Ruiz-Duenas, F. J. *Biochemistry* **2001**, *40*, 15660–15668.  
 (91) Ghering, A. B.; Jenkins, L. M.; Schenck, B. L.; Deo, S.; Mayer, R. A.; Pikaart, M. J.; Omichinski, J. G.; Godwin, H. A. *J. Am. Chem. Soc.* **2005**, *127*, 3751–3759.

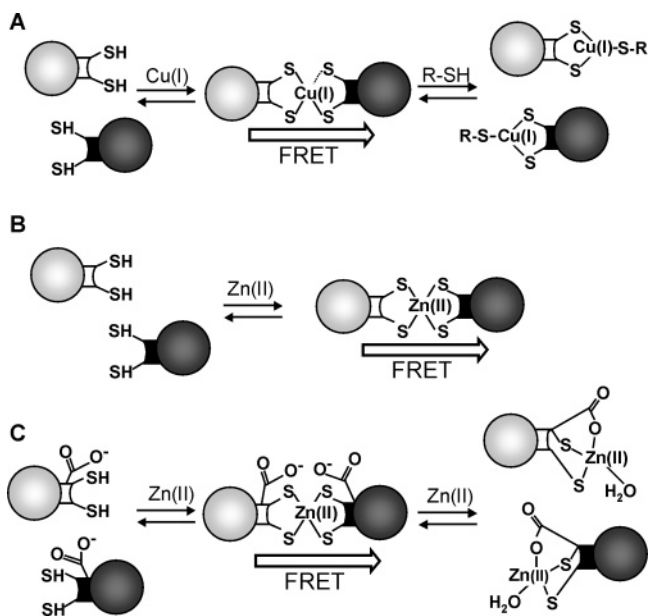


**Figure 7.** Mechanism explaining the different coordination modes observed for metal binding to CFP-Atox1 and WD4-YFP. (A) Addition of Cu(I) results in a Cu(I)-bridged dimer, but in the presence of free thiols a three-coordinate monomeric Cu(I) complex is more stable. (B) Addition of Zn(II) results in a metal-bridged dimer, with Zn(II) coordinated by four cysteines in a tetrahedral configuration. (C) Introduction of an extra Zn(II)-coordinating aspartate also allows the formation of a stable monomeric Zn(II) complex at higher Zn(II) concentrations. Please note that some of the metal ligands are likely to be protonated; these protons are not shown for clarity.

at least four ligands also explains our results for the MTCXXC-to-MDCXXC mutants. At low concentrations of Zn(II), the Zn(II)-bridged dimer is the most stable form, but addition of more Zn(II) results in the disruption of the dimer by binding of Zn(II) to each of the metal binding domains (Figure 7C). The NMR structure of ZntA, which binds Zn(II) in a single MDCXXC motif, shows a four-coordinated complex with Zn(II) bound via the two cysteines, one of the carboxylate oxygens, and water.<sup>35</sup> Interestingly, a dissociation constant of 20 nM has been determined for Zn(II) binding to ZntA, which is similar to the apparent dissociation constant for binding of the second Zn(II) in our system.<sup>92</sup>

The finding that Co(II) and Cd(II) also induce FRET is not surprising, since both metal ions are known to have coordination properties similar to those of Zn(II) and are often used as spectroscopic substitutes of the spectroscopically silent zinc.<sup>81</sup> Interestingly, Pb(II) also prefers to form a bridging complex. Many of the toxic effects of Pb(II) have been ascribed to its tendency to bind to Zn(II) sites in enzymes and transcription factors, in particular cysteine-rich sites.<sup>83,91</sup> Our finding that the Pb(II)-mediated interaction is readily disrupted by DTT indicates that Pb(II) is coordinated by only three cysteines, which confirms recent work that suggested that Pb(II) generally prefers coordination by three cysteines, whereas Zn(II) prefers four-coordination.<sup>82</sup> We are currently testing these hypotheses by studying the effect of single cysteine-to-serine mutations on the metal selectivity of the interaction.

Circular dichroism and X-ray absorption spectroscopy have previously been used to study the binding of Zn(II) to the

N-terminal domain of ATP7B. This study reported a stoichiometry of 6 Zn(II) ions per domain and ligation dominated by nitrogen ligands.<sup>93</sup> In this study we provide strong evidence for direct competition between Zn(II) and Cu(I) binding, however, since addition of Cu(I) in the presence of DTT disrupts the Zn(II)-mediated interaction. Moreover, mutation of the Cu(I)-binding cysteines to serines completely disrupts the Zn(II)-mediated Atox1-WD4 interaction. Our finding raises the interesting question whether Zn(II) binding to copper chaperone domains is physiologically relevant. Interestingly, preliminary yeast two-hybrid studies showed that the Atox1-WD4 interaction is indeed Zn(II)-dependent, as a 2-fold higher  $\beta$ -galactosidase activity was measured after addition of 300  $\mu$ M Zn(II) to the medium compared to the highest activity obtained for copper (Figure S5). Other examples of linked copper and zinc homeostasis are that both metals bind to metallothioneins<sup>33,34</sup> and the fact that Zn(II) supplementation is an effective treatment for patients with Wilson's disease, because it suppresses the accumulation of copper in the liver of these patients.<sup>94</sup>

The CFP-Atox1 and WD4-YFP pair has several properties that make it an attractive starting point for the development of a genetically encoded Zn(II) sensor. Important qualities for such a sensor include physiologically relevant affinity and selectivity, a concentration-independent fluorescent signal (ratiometric, anisotropy, lifetime), and control over intracellular localization and concentration. The intracellular Zn(II) concentration is actually not well established but may vary dramatically among organisms, cell types, and subcellular localization. The cytosolic concentration of Zn(II) in most mammalian cells has been estimated to be less than 1 nM,<sup>20,23,24,95</sup> but millimolar concentrations have been determined in synaptic vesicles in neuronal cells.<sup>96</sup> The zinc-specific transcriptional activator ZntR from *E. coli* binds Zn(II) with a  $K_d$  of  $1.6 \times 10^{-15}$  M, suggesting that the normal concentration of free Zn(II) in *E. coli* is 6 orders of magnitude lower than one ion per cell.<sup>21,22</sup> The Zn(II) affinity of CFP-Atox1/WD4-YFP is similar to that of the most sensitive zinc-specific dyes,<sup>45,48,55,59</sup> fluorescently labeled Zn-finger peptides,<sup>54,66,67</sup> and the carbonic anhydrase-based sensor developed by Thompson and co-workers.<sup>23,68</sup> Genetically encoded, GFP-based zinc sensors have also been reported previously, but these showed only a weak-to-moderate affinity for Zn(II).<sup>70</sup> Jensen and co-workers reported a ratiometric FRET-based system, in which introduction of Zn(II)-coordinating amino acids at the exterior of CFP and YFP allowed Zn(II) detection by the formation of Zn(II)-bridged CFP–YFP dimers. Although the principle is similar to our system, the affinity is 6 orders of magnitude lower with a  $K_d = 0.7$  mM.<sup>71</sup> The current CFP-Atox1/WD4-YFP system has two important drawbacks that currently limit its applicability for intracellular imaging. The ratio change observed upon Zn(II) binding is relatively small. Work on other FRET-based sensor systems has shown that similar ratio changes can be detected intracellularly, but these studies were done on a sensor in which donor and acceptor were part of a single protein chain.<sup>97</sup> Application of the current system

(93) DiDonato, M.; Zhang, J.; Que, L., Jr.; Sarkar, B. *J. Biol. Chem.* **2002**, *277*, 13409–13414.

(94) Brewer, G. J.; Yuzbasiyan-Gurkan, V.; Lee, D. Y.; Appelman, H. J. *Lab. Clin. Med.* **1989**, *114*, 633–638.

(95) Nasir, M. S.; Fahmi, C. J.; Suhay, D. A.; Kolodnick, K. J.; Singer, C. P.; O'Halloran, T. V. *J. Biol. Inorg. Chem.* **1999**, *4*, 775–783.

(96) Frederickson, C. J.; Suh, S. W.; Silva, D.; Thompson, R. B. *J. Nutr.* **2000**, *130*, 1471S–1483S.

(92) Liu, J.; Stemmler, A. J.; Fatima, J.; Mitra, B. *Biochemistry* **2005**, *44*, 5159–5167.



would require coexpression of two proteins at a 1:1 ratio, which is difficult to achieve in practice. To make the present sensor suitable for cellular zinc imaging, the two protein domains should be fused into a single protein via a flexible peptide linker. Such a single protein sensor would be easier to introduce into cells. In addition, linking the two domains could enhance the Zn(II) affinity and would make it independent of the protein concentration. Increasing the Zn(II) affinity relative to the Cu(I) affinity will be essential to obtain a reliable Zn(II) sensor without interference by Cu(I) binding. Finally, knowledge about the coordination preferences of Cu(I) and Zn(II) could be applied to further tune the affinity and selectivity of the metal binding site using site-directed mutagenesis. These mutations could include metal coordinating residues but also residues involved in docking to partner proteins in the Cu(I) transport pathway that would block in vivo Cu(I) loading.

## Conclusion

Fusion of cyan and yellow fluorescent protein domains to the copper binding domains Atox1 and WD4 yielded a ratio-metric fluorescent sensor for Cu(I) and Zn(II). Whereas the suitability as a Cu(I) sensor is limited due to its thiol sensitivity, this protein pair unexpectedly yielded a sensor with a subnanomolar affinity for Zn(II). The metal binding properties of this

system can be readily understood on the basis of the known coordination chemistries of Zn(II) and Cu(I). This study provided new insights into the mechanism of transition metal homeostasis, in particular on metal selectivity and the role of protein–protein interactions. The present system represents an attractive platform for the further development of genetically encoded FRET-based sensors for Zn(II).

**Acknowledgment.** We thank Toon Evers for expert assistance with fluorescence spectroscopy and for preparing illustrations, Marijn Vlaming for performing some initial experiments relevant to this work, Irene Kaashoek en Mattijs Elschot for performing  $\beta$ -galactosidase assays, and Marcel van Genderen for assistance with curve fitting procedures.

**Supporting Information Available:** Figures S1–S3 display the effect of EDTA and Zn(II) on the fluorescence spectra of CFP-WD4/Atox1-YFP, CFP-Atox1/Atox1-YFP, and CFP-WD4/WD4-YFP, respectively; Figure S4 shows competition between Cu(I) and Zn(II) binding as a function of Cu(I) concentration; and Figure S5 shows the effect of Zn(II) on the interaction between Atox1 and WD4 using yeast two-hybrid analysis. This material is available free of charge via the Internet at <http://pubs.acs.org>.

JA0610030

(97) Fehr, M.; Frommer, W. B.; Lalonde, S. *Proc. Natl. Acad. Sci. U.S.A.* **2002**, *99*, 9846–9851.